Time-lapse microscopy and classification of 2D human mesenchymal stem cells based on cell shape picks up myogenic from osteogenic and adipogenic differentiation

Christof Seiler[1], Amiq Gazdhar[2], Mauricio Reyes[1], Lorin M Benneker[3], Thomas Geiser[2], Klaus A Siebenrock[3] & Benjamin Gantenbein-Ritter[1,4]

[1] *Institute for Surgical Technology and Biomechanics, University of Bern, Bern, Switzerland*
[2]*Department of Pulmonary Medicine, Insel University Hospital, Bern, Switzerland*
[3]*Orthopeadic Department, Insel University Hospital, Bern, Switzerland*
[4]*ARTORG Center for Biomedical Engineering Research, University of Bern, Bern, Switzerland*

To: Journal of Tissue Engineering and Regenerative Medicine

Corresponding Author:
Prof. Dr. Benjamin Gantenbein
University of Bern
Medical Faculty
ARTORG Center for Biomedical Engineering Research
Institute for Surgical Technology and Biomechanics
Stauffacherstrasse 78
CH-3014 Bern
Tel +4131 631 5926
Fax +4131 631 5960
e-mail: benjamin.gantenbein@artorg.unibe.ch

This is the peer reviewed version of the following article: Seiler, C., Gazdhar, A., Reyes, M., Benneker, L. M., Geiser, T., Siebenrock, K. A., & Gantenbein-Ritter, B. (2014). Time-lapse microscopy and classification of 2D human mesenchymal stem cells based on cell shape picks up myogenic from osteogenic and adipogenic differentiation. Journal of Tissue Engineering and Regenerative Medicine, 8(9), 737-746, which has been published in final form at http://dx.doi.org/10.1002/term.1575. This article may be used for non-commercial purposes in accordance with Wiley Terms and Conditions for Use of Self-Archived Versions.

For Peer Review

Abstract

Current methods to characterize mesenchymal stem cells (MSCs) are limited to CD marker expression, plastic adherence and their ability to differentiate into adipo-, osteo- and chondrogenic precursors. It seems evident that stem cells undergoing differentiation should differ in many aspects such as morphology and possibly also in behavior, however such correlation has not yet being exploited for fate prediction of MSCs.

Primary human MSCs from bone marrow were expanded and pelleted to form high-density cultures and were then split/ (randomly divided) into four groups to differentiate into adipo-, osteo-, chondro-, and myogenic progenitor cells. Cells were expanded as heterogeneous and clonal populations and tracked with time-lapse microscopy to record cell shape using phase-contrast microscopy. Cells were segmented using a custom-made image processing pipeline. Seven morphological features were extracted for each of the segmented cells. Statistical analysis was performed on the 7-dimensional feature vectors using a tree-like classification method. Differentiation of cells was monitored with key marker genes and histology. Cells in differentiation media were expressing the key genes for each of the three pathways after 21 days, i.e. adipo-, osteo-, chondrogenesis, which was also confirmed by histological stains. Time-lapse microscopy data was obtained and contained new evidence that two cell shape features, eccentricity and filopodia (= “fingers”) are highly informative to classify myogenic differentiation from all others. However, no robust classifiers could be identified for the other cell differentiation paths.

Results suggest that non-invasive automated time-lapse microscopy could be potentially used to predict stem cell fate of hMSCs for clinical application based on morphology for earlier time-points. Classification is challenged by cell density, proliferation and possible unknown donor-specific factors, which affect the performance of morphology-based approaches.

Keywords. time-lapse microscopy, mesenchymal stem cells, real-time RT-PCR, histology, segmentation, cell shape, filopodia

For Peer Review

http://mc.manuscriptcentral.com/term

1. Introduction

Autologous human mesenchymal stem cells (hMSCs) have been proposed as a major source for regenerative therapy for the musculoskeletal system (Giordano *et al.* 2007; Caplan 1991; Pittenger 2008; Chamberlain 2006; Prockop 1997; Prockop 2001). The reason for this is three-fold. First, these cells can be isolated from the human body (bone-marrow, adipose tissue). Second, these cells are fast expanded *in vitro* (Caplan 1991; Pittenger *et al.* 1999; Caplan 2005). Third, there is no ethical controversy. The natural stem-cell "niche" of these cells, however, has not been described in detail and current laboratory practice is to expand these cells as a mixed and heterogenous cell population, starting from few founder cells (Chamberlain 2006; da Silva Meirelles *et al.* 2008). The International Society for Cellular Therapy defined the minimal standards for a stromal cell population to be called "hMSCs": First, MSCs must be plastic-adherent when maintained in standard culture conditions. Second, MSCs must express CD105, CD73 and CD90, and lack expression of CD45, CD34, CD14 or CD11b, CD79a or CD19 and HLA-DR surface molecules. Third, MSCs must differentiate to osteoblasts, adipocytes and chondroblasts *in vitro* (Dominici *et al.* 2006). However, this definition still does not define the source pool of these cell populations nor does it tell about the heterogeneity of these cells and also its outcome. hMSCs have attracted immense research interest in the field of regenerative medicine due to their ability to be cultured for successive passages and multi-lineage differentiation. However, the molecular mechanisms governing MSCs self-renewal and differentiation remain largely unknown. The self-renewal capability of MSCs was only recently proven with "true single cell clonal tracing" of lineages (Sarugaser *et al.* 2009). However, the heterogenic nature of these stem cell populations have been noted to be a major source of variance (Sengers *et al.* 2009; Solchaga *et al.* 1999; Roeder and Radtke 2009). The development of sophisticated techniques, in particular clinical proteomics, has enabled researchers in various fields to identify and characterize cell specific biomarkers for therapeutic purposes. For instance, a recent study tried to understand the cellular and sub-cellular processes responsible for the existence of stem cell populations in bone marrow samples by revealing the whole cell proteome of the clonal cultures of bone marrow-derived MSCs (Mareddy *et al.* 2009). However, all of these methods require to invasively manipulate these cells and to use some sort of labeling or real-time reverse transcription (RT) PCR techniques to confirm the phenotype of these cells for down-stream analyses or direct clinical

For Peer Review

application. Clinical application to inject these expanded cells in any tissue such as the intervertebral disc would require prior knowledge about the differentiation state of these cells (Dainiak *et al.* 2007). Here, we propose to characterize hMSCs without direct invasive manipulation of these cells using an approach herewith termed "statistical stem cell" modeling, involving microscopic imaging and advanced image processing algorithms. The primary aim of this study was to observe the shape of primary human mesenchymal stem cells undergoing differentiation on standard culture plastic under *in vitro* controlled conditions and to evaluate any correlations between shape of stem cells, cell type and differentiation pathways. Hence, here we evaluate any correlations between shape of stem cells and the fate during the differentiation process of primary human MSCs in 2D cell culture.

2. Materials and methods

2.1 Cell source and expansion

Human bone marrow was harvested from a patient undergoing hip or spine surgery with written consent. The procedure was approved by the local Ethics Office (KEK # 187/10). Human mesenchymal stem cells (hMSCs) were amplified from "buffy coat" after density gradient centrifugation by selection for plastic adherence. Passage 3 cells were seeded onto standard plastic culture plates (Falcon, VWR, Switzerland) in inductive media for osteogenic, adipogenic, myogenic, 3D alginate chondrogenic (not live tracked) and control and kept in culture for 21 days. The time-lapse imaging was conducted with IncuCyte Plus® (Essen BioScience, Bucher, Switzerland) for 6 days. At the end of experiments cell phenotype during differentiation was monitored by real time RT-PCR analysis of key genes such as transcription factors, which are characteristic for osteogenic, adipogenic, myogenic and chondrogenic pathways.

2.2 CD marker characterization

Cells were trypsinized and resuspended in phosphate buffered saline (PBS) containing 0.5% bovine serum albumin (BSA), and were stained with the antibodies as given in Table 1. 2 µl of antibody reaction solution, as provided from the manufacturer (Becton Dickinson and Company, Allschwil, Switzerland) was added to 2.5 x 10^5 cells and incubated for 30 min with the cells. The antibodies were then removed and the cells were washed with PBS containing 0.5% bovine serum albumin (BSA) and kept therein until measured. Cells were characterized on a BD™ LSR II (BD

For Peer Review

Pharmagen, Brussels, Belgium) using fore-scatter, side-scatter and the lasers for the specific dyes, FITC, PE, AlexaFluor 488, PE-Cy5 and PE-Cy7 (Table 1).

2.3. *Stem Cell Differentiation*

Primary human mesenchymal stem cells were passaged and ~10^4 cells were seeded into 6-well plates and let grow and differentiate for up to 21 days. For chondrogenic differentiation the cells were seeded in 1.2% alginate (Fluka, Sigma Aldrich, Buchs, Switzerland) with 4M cells / mL (Mehlhorn *et al.* 2006; Gantenbein-Ritter *et al.* 2011). Beads were produced by steadily pressing cell suspension through a syringe equipped with a 22G needle into 102mM $CaCl_2$ 0.9% NaCl solution, as previously described (Gantenbein-Ritter *et al.* 2011).

The stem cells were differentiated in the following media (treatments): Adipogenic induction medium (AIM): consisting of α-Modified Eagles Medium (αMEM) containing 10% fetal bovine serum (FBS), antibiotics, 0.5mM methyl-isobutylxanthine, 1µM dexamethasone and, 10 µg/mL insulin and 100 µM indomethacin.

Chondrogenic differentiation medium (CHDM) consisted of high glucose (4.5g/L) DMEM supplemented with 6.25µg/mL insulin, 6.25µg/mL transferrin, 6.25µg/mL selenous acid, 5.33 µg/mL γ-linoleic acid, and 1.25 mg/mL bovine serum albumin (ITS+, Sigma-Aldrich, Buchs, Switzerland), 0.1µM dexamethasone, 10 ng/mL transforming growth factor β1 (TGF-β1, Peprotech, London, UK), 50 µg/mL ascorbate 2-phosphate, 2 mM pyruvate, and antibiotics. HMSCs were seeded in 1.2% alginate (Fluka, Sigma-Aldrich, Buchs, Switzerland) at a density of 4x10^6 cells/ml.

Osteogenic supplemented medium (OSM): DMEM with 10% fetal calf serum with osteogenic supplements 50 µM ascorbate 2-phosphate, 10 mM -glycerol phosphate, and 100 nM dexamethasone. Myogenic medium (MYM): Induced cells were placed in myogenic supplemented (MS) media comprising 88% α-MEM, 10% antibiotics, 10% FBS, 1 nM dexamethasone (Sigma-Aldrich), and 2µM hydrocortisone (Sigma-Aldrich). The culture medium was replaced every 3 days until multinucleated myotubes could be observed (28 days).

2.4. Time-lapse microscopy settings

The cells of the heterogenous hMSCs population were monitored with an Incucyte Plus® time-lapse microscope, which was put into a standard incubator at 5% CO_2,

http://mc.manuscriptcentral.com/term

For Peer Review

95% humidity. The software of the microscope was configured to take an image of each well every 2h from the start of the differentiation experiment, i.e. the imaging started after ~20 min after seeding the cells and was then continued for 6 days, with a 20 min break for media refreshment after 3 days. This covered the exponential growing phase until confluence. The data was collected as tiff images and processed with a customized image pipeline as described below.

2.5. *Analysis of time-lapse microscopy data and segmentation algorithms*

Differentiation of cells was monitored with key marker genes and histology. Cells were segmented using a custom-made image processing pipeline. The segmentation pipeline was implemented in order to distinguish cells from the background. The segmentation pipeline is composed of standard image processing operations in the following order: 1) original image (Figure 1.1), 2) Sobel edge detection (Figure 1.2), 3) image dilation (Figure 1.3), 4) removal of objects close to image borders (Figure 1.4), 5) image erosion (Figure 1.5), 6) removal of small objects (Figure 1.6), 7) filling of gaps inside the cell (Figure 1.7) and 8) overlay of the final result on the original image (Figure 1.8). Seven morphological features were extracted from each of the segmented cells. The feature space in which we performed statistical classification was therefore 7-dimensional (one vector for each cell), with the following features: Area, major and minor axis length, perimeter, eccentricity, extent, and number of fingers. Statistical analysis was performed on the 7-dimensional feature vectors using a tree-like classification method called the Node Harvest method, which was introduced by (Meinshausen 2009). The developed Matlab™ and R routines are available at http://www.mathworks.ch/matlabcentral/fileexchange/ on the webpage of Mathworks inc. under the project name "cell shape classifier".

2.6. Feature vector

Once the cells were segmented we extracted the following 7-dimensional feature vector (Figure 2): 1) **Area:** The number of pixels of a cell. 2) **Major axis length:** Scalar specifying the length (in pixels) of the major axis of a cell. 3) **Minor axis length:** The length (in pixels) of the minor axis of a cell. 4) **Perimeter:** The distance around the boundary of a cell. 5) **Eccentricity:** Scalar that specifies the eccentricity of the cell. The eccentricity is the ratio of the distance between the foci of the cell and its major axis length. The value ranges from 0 to 1, where 0 represents circular shaped

For Peer Review

cells and 1 cells that are stretched out to a line. 6) **Extent:** Scalar that specifies the ratio of pixels inside the cell to pixels in the enclosing box. 7) **Finger:** Thresholded result of the Poisson equation with boundary condition set to zero at contour of the cell. In Gorelick *et al.* (2006) the authors used the same algorithm to identify human fingers. Here, we took advantage of the analogy between human fingers and cell "fingers".

2.7. Statistical Analysis using Node Harvest

We applied the Node Harvest (Meinshausen 2009) method to classify feature vectors. Node harvest is a statistical classification technique that combines interpretability and prediction accuracy, and is especially suited for low signal-to-noise data due to its robust estimation process.

Node Harvest starts by randomly generating a few thousands nodes. Each node represents a set of observations, in our case the cells, and a set of conditions, in our case elements of the feature vector. For instance in Figure 6B, the node on the bottom right contains 720 cells (y-axis) with the property 0.96 <= Eccentricity. The size of the node indicates the importance, which is found through a new type of optimization algorithm favoring sparse solutions. The sparseness reduces the number of nodes in the final plot and enables better interpretability. The connection between nodes represents subsets. Finally, on the x-axis the likelihood of one cell belonging to one cell type is shown, as we can see there is no discrete classification but a continuous classification indicating the likelihood of assignment to either one of the cell types. The only parameter to define is the number of nodes that are randomly generate at the beginning. We obtained stable results by using 1000 nodes. Further it is possible to constrain the maximum number of conditions per node, we chose one condition per node to maximize interpretability (Meinshausen 2009).

2.8. Real time RT-PCR

The differentiation process was monitored using "key genes" for the mesenchymal differentiation, i.e. adipogenic, osteogenesis, chondrogenesis and myogenesis. The primers were designed using Beacon designer software (Premier Biosoft inc., Palo Alto, CA, USA), synthesized at Microsynth (Balgach, Switzerland), and tested for efficiency (around 100%) before using in the experiment (Table 3). Real-time gene expression was monitored and the ribosomal 18S was used as a reference gene (Livak

For Peer Review

and Schmittgen 2001; Schmittgen and Zakrajsek 2000). Around 500ng of total RNA was reverse-transcribed using the iScript kit (Bio-Rad, Basel, Switzerland). Real-time PCR was then carried out mixing 5µl of the 5x (in 1x Tris-EDTA buffer) diluted cDNA and the IQ SYBR Green Supermix (Bio-Rad) on an IQ5 cycler from Bio-Rad. The 2-step amplification profile was 45 cycles (95° for 15s and 61°C for 30s). All amplicons were analyzed using melting curve analysis for the presence of pseudo genes. Relative gene expression was first calculated relative to reference gene as ΔC_t values. The relative gene expression was analyzed using the $2^{-\Delta\Delta Ct}$ method (Livak and Schmittgen 2001) and relative to the undifferentiated cells of day 0.

2.9. Histology

The cells were initially fixed in 4% paraformaldehyde (PFA) directly on the 6-well plate and stored at 4°C prior staining. Cells were then rinsed in PBS and then stained for Red Oil and Meyer's haematoxilin or for nuclear fast red and Von Kossa silver stain (Osteogenic pathway)(Zuk *et al.* 2001). For myogenic differentiation, cells were transferred after 14 days onto glass cover slips in 6-well plates and let grow for 72 h and then fixed in 3.7% formalin for immunostaining staining along with its uninduced negative controls. For immuno-histochemistry, fixed cells were first permeabilized with 100% methanol for 2 minutes, and blocked with 10% FBS/PBS for 1 hour. The cells were then incubated with mouse-anti-human MyoD primary antibody (Santa Cruz biotech, Santa Cruz, CA, USA) or rabbit-anti-human α-SMA (smooth muscle actin (A2066, Sigma Aldrich). After washing, the cells were incubated for 1 h with goat-anti-mouse Alexa Fluor 555 IgG_1 secondary antibody (Molecular Probes, Invitrogen, Basel, Switzerland) or with goat-anti-rabbit FITC (ab 6717, Abcam USA,) for α-SMA and then incubated for 1 hour in 0.5% BSA PBS and washed thoroughly. Cover slips were mounted in slow-fade gold embedding medium with DAPI (Molecular Probes). Cells were then imaged with a confocal laser scanning microscope (cLSM 510, Carl Zeiss, Jena, Germany).

3. Results

3.1. CD Marker Characterization

The primary cells at passage 3 were homogeneously positive for CD44, CD105, CD90 and negative for CD14, CD34 and CD45 (data not shown).

http://mc.manuscriptcentral.com/term

For Peer Review

3.2. Stem Cell Differentiation

Primary human mesenchymal stem cells could be differentiated into osteogenetic, adipogenetic and chondrogenic progenitor cells (Figures 3-5). The cells were differentiating into the four lineages as detected by relative gene expression of key marker genes (Figure 3) and could also be stained for osteogenic (black calcium deposition) adipogenic (presence of red oil droplets), starting from day 9 (Figure 4). The adipogenic pathway could be confirmed by the onset of adiponectin (APN) expression (upregulation by a factor of 2,000 times, Figure 3). Osteogenic differentiation was found by an increase of osteopontin (OPN). The relative gene expression levels of collagen type I and osteocalcin (OSC), however, were not considerably different from the levels of the undifferentiated stem cells. Nevertheless, the complete absence of calcium deposits in negative controls (expansion medium and with adipogenic medium, data not shown) could be confirmed using a histological staining for Von Kossa calcium deposition. Chondrogenic differentiation could be demonstrated by the significant up-regulation of aggrecan (by a factor of 1,000) and by the up-regulation of collagen type 2 (by a factor of 10^6, Figure 3), as well as an increase in alcian blue stain (Figure 4). Finally, myogenic differentiation was checked by the expression of myosin heavy chain (MyoD), which is a transcription factor for myogenesis and of the gene desmin (DES), a gene that encodes a muscle-specific class III intermediate filament). MyoD and α-sm actin were also found positively stained by immunohistochemistry, which further confirmed the myogenic differentiation (Figure 5).

3.3. Node Harvest

The Node Harvest algorithm clustered the cells into two branches (Figure 6A-D). Eccentricity (Figure 6A-C) has been picked up to be the main classifier for the myogenic differentiation as well as "fingers", i.e. filopodia (Figure 6 D). Fingers were important to distinguish myogenic versus all other cell differentiations, i.e. Control, adipo- and osteogenic. No clusters have been identified for the other three differentiation groups if compared to all others (data not shown).

4. Discussion

4.1. Differentiation of Stem Cells and Correlation with Cell Shape

For Peer Review

It seems evident that expansion of primary cells is a crucial step for the application of stem cell therapy (Majd *et al.* 2008; Sarugaser *et al.* 2009; da Silva Meirelles *et al.* 2008).

Here we demonstrate that modern time-lapse microscopy could be a potential tool to predict stem cell fate (Lutolf *et al.* 2009). We could successfully sort out the myogenic differentiation pattern from the, adipogenic, osteogenic and undifferentiated control cells, based solely on morphological feature vector. We could demonstrate that with the onset of myogenic differentiation (during the first 48hrs of cell expansion) primary hMSCs undergo changes in eccentricity and cells undergoing myogenic fusion have an increased number of "filopodia". The two features "eccentricity" and "finger" (= filopodia) were significantly higher in the early myogenic differentiation as compared to all other groups, as picked up by the Meinshausen classification algorithm (Meinshausen 2009). Of course, cell shape can change by a large number of reasons; change in pH, limited nutrition, changes in osmolality, cell density, and possibly others. However, over a large set of cells and in a controlled environment, such as lab standard plastics, it should be feasible to predict an average cell type using the proposed statistical stem cell methodology.

Furthermore, it is known that primary hMSCs are always a heterogenous cell population. Although our cells possessed the typical CD markers on their cell surface, as expected for stromal cells at the third passage, it is of course obvious that various phenotypes of stem cells might still be present in the populations and causing high variance of cell shapes. Also the ratio between differentiated and undifferentiated cells might run at different speed among the four differentiation groups. The application of reporter systems is a very useful tool to visualize the reorganization of the cells. However, transfection of cells with a CytoMegalovirus (CMV) promoter based expression system might of course influence the behavior and thus the shape of primary cells (Raimondo *et al.* 2006). Here, the development of a negative reporter system for *nanog* could be very helpful tool to distinguish undifferentiated cell from those undergoing differentiation (Pierantozzi *et al.* 2010).

4.2. Cell Classification Pipeline

There are three parts to the classification pipeline: segmentation, feature selection and classification. The performance of each part depends on the performance of the previous one.

http://mc.manuscriptcentral.com/term

For Peer Review

In the segmentation step, we did not consider the time of acquisition associated with each image. By tracking cells over time we could potentially improve the robustness of our cell segmentation algorithm (Gilbert *et al.* 2010). However, we noticed that taking a picture every 2h is not enough to trace individual hMSCs over time as has been recently proposed (*Gilbert et al*. 2010). This was not possible with the chosen time-lapse microscope set-up. Cell density certainly affected cell shape, a factor, which was considered by our segmentation routine by excluding cells, which were connected to the edges of the images.

In the feature selection step, we could consider more morphological parameters or even intensity patterns. Furthermore, we believe that stem cell fate prediction can be enhanced by taking into account different scales of modelling, considering not only local characteristics of cell shape but also their interaction with and within a group of neighbouring cells (i.e. from individual to group modelling).

In the classification step, we chose a robust technique that is easy to interpret, which, given the nature of our data, is a reasonable choice. To get a relative performance measure it would be interesting to compare it to other methods such as tree clustering methods (Morris *et al.* 2011).

4.3. Cell Shape Predictors

Other approaches to characterize change in cell shape were followed in other works. For instance, (Glauche *et al.* 2009) attempted to quantify changes in tree topologies using mother-daughter cell phylogenies or (Cohen *et al.* 2010; Ravin *et al.* 2008) by application of a relatively well-defined differentiation process of neuronal precursor cells. Klauschen *et al.* (2009) recently attempted to reconstruct cell surface modifications to predict cell shape in 3D. Two-dimensional cell tracking seems a relatively easy approach to undertake (Gilbert *et al.* 2010). Our study is limited in the sense that we did not extensively clone bone-marrow cells by limiting dilution to exclude further variance of cell shape caused by cell population mixture (Mareddy *et al.* 2007). In contrast, our primary aim was to test the feasibility to predict differentiation solely by means of non-invasive image processing of cell shape. The limitation is the high cell density culture as it is obtained for confluence > 70%. Future experiments should involve cell cycle synchronization during differentiation by hydroxyurea or colchicine in order to sort out cell shape changes from cell division (Lee *et al.* 2011; Banfalvi 2011). Another approach to predict stem cell fate non-

For Peer Review

invasively might be to use membrane polarity. Recently, it has been noticed that undifferentiated and differentiated cells differ in their polarity (Sundelacruz *et al.* 2009; Flanagan *et al.* 2008; Levin 2007). Undifferentiated cells have different "fate potentials" than differentiated cells (Flanagan *et al.* 2008). It remains to be shown whether human MSCs can be discriminated by different dielectric properties and whether the change in potential is a unique feature of each of the mesenchymal differentiation pathways (Sundelacruz *et al.* 2008). Possibly a combination of image processing techniques together with recording of membrane potential could be the most promising step towards non-invasive prediction of stem cell fate.

Conclusions

In this work, we demonstrated the potential to distinguish hMSCs differentiation from others through a classification of 7-dimensional feature vectors extracted from cells obtained from non-invasive time-lapse microscopy. In particular, the proposed segmentation pipeline and the node harvest classification algorithm picked up myogenic from all other cell differentiation pathways, which is prominent in pairwise comparisons (Figure 6). It remains to be shown whether this classification approach works out for large data sets, including donor variation and different cell sources (i.e., adipose, bone marrow). Other features have not been successfully identified to discriminate osteo-progenitor cells from adipose cells. With new time-lapse technologies emerging and more high-throughput data collection, new options to follow cells is possible. In addition, tracking cells in 3D opens new future challenges and possibilities.

Competing interests

The authors declare that they have no competing interests.

Acknowledgements

Ladina Ettinger and Elena Calandriello assisted in histological staining. Rainer Egli provided protocols for CD marker characterization of hMSCs.

List of abbreviations

αMEM: Minimum Essential Medium; AIM: Adipogenic induction medium; bFGF-2: basic fibroblast growth factor – 2; CD: cluster of differentiation; CHDM:

http://mc.manuscriptcentral.com/term

For Peer Review

Chondrogenic differentiation medium; CMV: Cytomegalo-Virus; DMEM: Dulbecco's modified Eagle's medium; hMSC: human Mesenchymal Stem Cell; IVD: Intervertebral Disc; MYM: Myogenic medium

References

Banfalvi, G. 2011; Overview of cell synchronization. *Methods Mol Biol* **761** 1-23.

Caplan, AI. 1991; Mesenchymal stem cells. *J Orthop Res* **9**(5): 641-650.

Caplan, AI. 2005; Review: mesenchymal stem cells: cell-based reconstructive therapy in orthopedics. *Tissue Eng* **11**(7-8): 1198-1211.

Chamberlain, JS. 2006; Stem-cell biology: a move in the right direction. *Nature* **444**(7119): 552-553.

Cohen, AR, Gomes, FL, Roysam, B, *et al.* 2010; Computational prediction of neural progenitor cell fates. *Nat Methods* **7**(3): 213-218.

Dainiak, MB, Kumar, A, Galaev, IY, *et al.* 2007; Methods in cell separations. *Adv Biochem Eng Biotechnol* **106** 1-18.

da Silva Meirelles, L, Caplan, AI, Nardi, NB. 2008; In search of the in vivo identity of mesenchymal stem cells. *Stem Cells* **26**(9): 2287-2299.

Dominici, M, Blanc, KL, Mueller, I, *et al.* 2006; Minimal criteria for defining multipotent mesenchymal stromal cells. The International Society for Cellular Therapy position statement. *Cytotherapy* **8**(4): 315-315.

Flanagan, LA, Lu, J, Wang, L, *et al.* 2008; Unique dielectric properties distinguish stem cells and their differentiated progeny. *Stem Cells* **26**(3): 656-665.

Gantenbein-Ritter, B, Benneker, LM, Alini, M, *et al.* 2011; Differential response of human bone marrow stromal cells to either TGF-β(1) or rhGDF-5. *Eur Spine J* **20** 962-971.

Gilbert, PM, Havenstrite, KL, Magnusson, KE, *et al.* 2010; Substrate Elasticity Regulates Skeletal Muscle Stem Cell Self-Renewal in Culture. *Science* **329**(5995): 1078-1081.

Giordano, A, Galderisi, U, Marino, IR. 2007; From the laboratory bench to the patient's bedside: an update on clinical trials with mesenchymal stem cells. *J Cell Physiol* **211**(1): 27-35.

Glauche, I, Lorenz, R, Hasenclever, D, *et al.* 2009; A novel view on stem cell development: analysing the shape of cellular genealogies. *Cell Prolif* **42**(2): 248-263.

Gorelick, L, Galun, M, Sharon, E, *et al.* 2006; Shape representation and classification using the poisson equation. *IEEE Trans Pattern Anal Mach Intell* **28**(12): 1991-2005.

Klauschen, F, Qi, H, Egen, JG, *et al.* 2009; Computational reconstruction of cell and tissue surfaces for modeling and data analysis. *Nat Protoc* **4**(7): 1006-1012.

Lee, WC, Bhagat, AA, Huang, S, *et al.* 2011; High-throughput cell cycle synchronization using inertial forces in spiral microchannels. *Lab Chip* **11**(7): 1359-1367.

Levin, M. 2007; Large-scale biophysics: ion flows and regeneration. *Trends Cell Biol* **17**(6): 261-270.

Livak, KJ, Schmittgen, TD. 2001; Analysis of relative gene expression data using real-time quantitative PCR and the 2^(-Delta Delta C(T)) Method. *Methods* **25**(4): 402-408.

For Peer Review

http://mc.manuscriptcentral.com/term

Lutolf, MP, Gilbert, PM, Blau, HM. 2009; Designing materials to direct stem-cell fate. *Nature* **462**(7272): 433-441.

Majd, H, Wipff, PJ, Buscemi, L, *et al.* 2008; A Novel Method of Dynamic Culture Surface Expansion Improves Mesenchymal Stem Cell Proliferation and Phenotype. *Stem Cells* **27**(1): 200-209.

Mareddy, S, Broadbent, J, Crawford, R, *et al.* 2009; Proteomic profiling of distinct clonal populations of bone marrow mesenchymal stem cells. *J Cell Biochem* **106**(5): 776-786.

Mareddy, S, Crawford, R, Brooke, G, *et al.* 2007; Clonal isolation and characterization of bone marrow stromal cells from patients with osteoarthritis. *Tissue Eng* **13**(4): 819-829.

Mehlhorn, AT, Schmal, H, Kaiser, S, *et al.* 2006; Mesenchymal stem cells maintain TGF-beta-mediated chondrogenic phenotype in alginate bead culture. *Tissue Eng* **12**(6): 1393-1403.

Meinshausen, N. 2009; Node harvest: simple and interpretable regression and classification. *Electronic Journal of Statistics* **arXiv** 0910.2145v1.

Morris JH, Apeltsin L, Newman AM, *et al.* 2011; clusterMaker: a multi-algorithm clustering plugin for Cytoscape. *BMC Bioinformatics* **12**: 436.

Pierantozzi, E, Gava, B, Manini, I, *et al.* 2010; Pluripotency Regulators in Human Mesenchymal Stem Cells: Expression of NANOG But Not of OCT-4 and SOX-2. *Stem Cells Dev* **20**(5): 915-923.

Pittenger, MF. 2008; Mesenchymal stem cells from adult bone marrow. *Methods Mol Biol* **449** 27-44.

Pittenger, MF, Mackay, AM, Beck, SC, *et al.* 1999; Multilineage Potential of Adult Human Mesenchymal Stem Cells. *Science* **284**(5411): 143.

Prockop, DJ. 1997; Marrow stromal cells as stem cells for nonhematopoietic tissues. *Science* **276**(5309): 71-74.

Prockop, DJ. 2001; Stem cell research has only just begun. *Science* **293**(5528): 211-212.

Raimondo, S, Penna, C, Pagliaro, P, *et al.* 2006; Morphological characterization of GFP stably transfected adult mesenchymal bone marrow stem cells. *J Anat* **208**(1): 3.

Ravin, R, Hoeppner, DJ, Munno, DM, *et al.* 2008; Potency and fate specification in CNS stem cell populations in vitro. *Cell Stem Cell* **3**(6): 670-680.

Roeder, I, Radtke, F. 2009; Stem cell biology meets systems biology. *Development* **136**(21): 3525-3530.

Sarugaser, R, Hanoun, L, Keating, A, *et al.* 2009; Human mesenchymal stem cells self-renew and differentiate according to a deterministic hierarchy. *PLoS ONE* **4**(8): e6498.

Schmittgen, TD, Zakrajsek, BA. 2000; Effect of experimental treatment on housekeeping gene expression: validation by real-time, quantitative RT-PCR. *J Biochem Biophys Methods* **46**(1-2): 69-81.

Sengers, BG, Dawson, JI, Oreffo, RO. 2009; Characterisation of Human Bone Marrow Stromal Cell heterogeneity for skeletal regeneration strategies using a two-stage colony assay and computational modeling. *Bone* **46**(2): 496-503.

Solchaga, LA, Johnstone, B, Yoo, JU, *et al.* 1999; High variability in rabbit bone marrow-derived mesenchymal cell preparations. *Cell Transplant* **8**(5): 511-519.

Sundelacruz, S, Levin, M, Kaplan, DL. 2008; Membrane potential controls adipogenic and osteogenic differentiation of mesenchymal stem cells. *PLoS ONE* **3**(11): e3737.

For Peer Review

1 Sundelacruz, S, Levin, M, Kaplan, DL. 2009; Role of membrane potential in the
2 regulation of cell proliferation and differentiation. *Stem Cell Rev Rep* **5**(3): 231-
3 246.
4 Zuk, PA, Zhu, M, Mizuno, H, *et al.* 2001; Multilineage cells from human adipose
5 tissue: implications for cell-based therapies. *Tissue Eng* **7**(2): 211-228.
6

For Peer Review

Figure legends

Figure 1. A-H Illustration of the segmentation pipeline that was used to extract cells from phase-contrast images. 10x magnification of the phase-contrast images. The time-lapse microscope series (microscope, Incucyte, Essen Bioscience) was used.

Figure 2. A-H The seven shape features that were extracted from each cell for morphological analysis.

Figure 3. Relative gene expression profiles for marker genes grouped for osteogenic, adipogenic, chondrogenic and myogenic differentiation of human mesenchymal stem cells (hMSCs).

Figure 4. Histological stainings for each of the four differentiation lines of primary human mesenchymal stem cells after 12, 15 and 21 days. First, column: Osteogenic differentiation: Von Kossa /fast red stain, second column: adipogenic differentiation, red oils / Meyer's hematoxylin, third and forth column: chondrogenic differentiation aclian blue and safranin O / fast green stain.

Figure 5. Confocal laser scanning microscope images of MyoD stain (ALEXA555) and for α-smooth muscle actin stain (FITC) for myogenic differentiation and negative controls. Nuclei were counter stained with DAPI. A. and B myotube formation after 14 days of culture which express MyoD, C is negative control and D is positive stain for undifferentiated control, E is positive staining for α smooth muscle (sm) actin of myogenic differentiation and F is negative control.

Figure 6. Output of Node Harvest classification method. The response axis represents **A:** myogenic=0 and control=1, **B:** myogenic=0 and adipogenic=1, **C:** myogenic=0 and osteogenic=1, **D:** myogenic=0 and adipgenic/osteogenic/control=1, where values between 0 and 1 represent a weighted combination of both types. The sample axis indicates the number of cells. Each node contains cells that fulfil one condition of one element of the 7-feature vector. The node size shows the relevance of that condition. Lines between nodes symbolize subsets.

For Peer Review

Table 1. Table of analyzed parameters to identify multi-potentiality of isolated plastic-adherent human mesenchymal stem cells (hMSCs).

Pathway	Gene Expression	Histology
Osteogenesis	col 1, OPN,	Von Kossa / Fast Red
Adipogenesis	Adiponectin	Red Oil /Meyer's hematoxilin
Chondrogenesis	ACAN, col2	Safranin O/Fast Green Alcian Blue
Myogenesis	MyoD, Desmin	α-sm actin, MyoD

For Peer Review

Table 2. Labelled Antibodies for Characterization of primary human Mesenchymal Stem Cells (hMSCs).

Antigen	Synonym	Supplier	Cat.No.	Fluorophore	Isotype
CD44	Hyaluronan receptor	BD Pharmingen	555478	FITC	mouse IgG2b, □
CD90	Thy-1glycophosphatidylinositol (GPI) anchored conserved cell surface protein	BD Pharmingen	555595	FITC	mouse IgG1, □
CD34	Important adhesion molecule for T-lymphocytes	BD Pharmingen	555823	PE-Cy5	mouse IgG1, □
CD45	Leukocyte common antigen	BD Pharmingen	557748	PE-Cy7	mouse IgG1, □
CD105	Endoglin	Invitrogen	MHCD10520	AlexaFluor 488	mouse IgG1, □
CD14	Monocyte differentiation antigen	BD Pharmingen	557742	PE-Cy7	mouse IgG2a, □

Remark: The sign, which is not shown in PDF is “kappa”

http://mc.manuscriptcentral.com/term

Table 3 Real-time RT-PCR Primers used for Real-time RT-PCR. All primers were run at 61°C T_a (annealing temperature) and a two-step protocol.

Gene Abbreviation	Name	Forward	Reverse
Hs18S	Reference Gene	CGA TGC GGC GGC GTT ATT C	TCT GTC AAT CCT GTC CGT GTC C
Chondrogenic Differentiation			
ACAN	Aggrecan core protein	CAT CAC TGC AGC TGT CAC	AGC AGC ACT ACC TCC TTC
col1A2	Collagen 1 A2	GTG GCA GTG ATG GAA GTG	CAC CAG TAA GGC CGT TTG
col2A1	Collagen 2 A1	AGC AAG AGC AAG GAG AAG	GGG AGC CAG ATT GTC ATC
Osteogenic Differentiation			
OSC	Osteocalcin	GCA GAG TCC AGC AAA GGTG	CCA GCC ATT GATA CAG GTA GC
OPN	Osteopontin	ACG CCG ACC AAG GAA AAC TC	GTC CATA AAC CAC ACT ATC ACC TCG
Adipogenic Differentiation			
APN	Adiponectin	CCG TGA TGG CAG AGA TGG	TATA CATA GGC ACC TTC TCC AG
Myogenic Differentiation			
MyoD	Myosin heavy chain	ACA ACG GAC GAC TTC TAT	GTG CTC TTC GGG TTT CAG
DES	Desmin (BD)	GCA GCC AAC AAG AAC AAC	CAA TCT CGC AGG TGT AGG

For Review

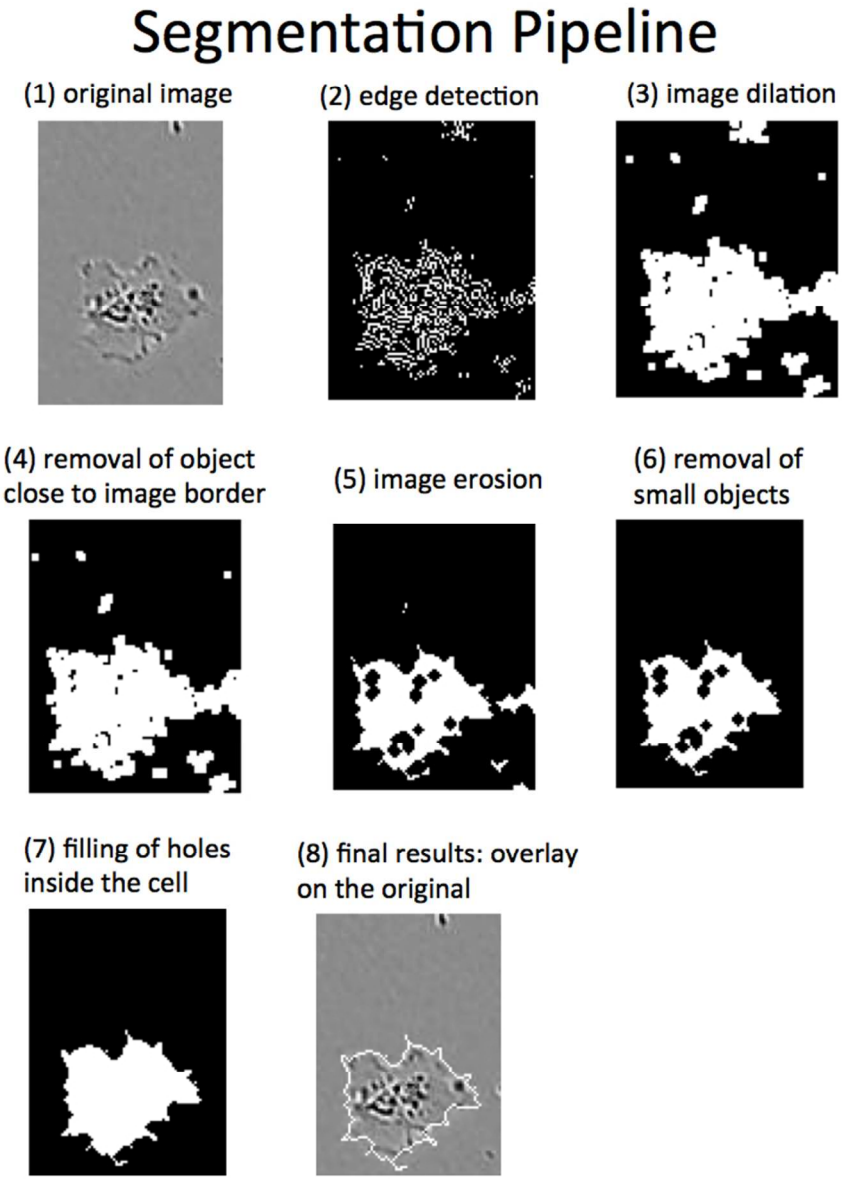

Figure 1. A-H Segmentation pipeline that was used to extract shape from phase-contrast images using the 10x magnification of the time-lapse microscope images.
130x171mm (150 x 150 DPI)

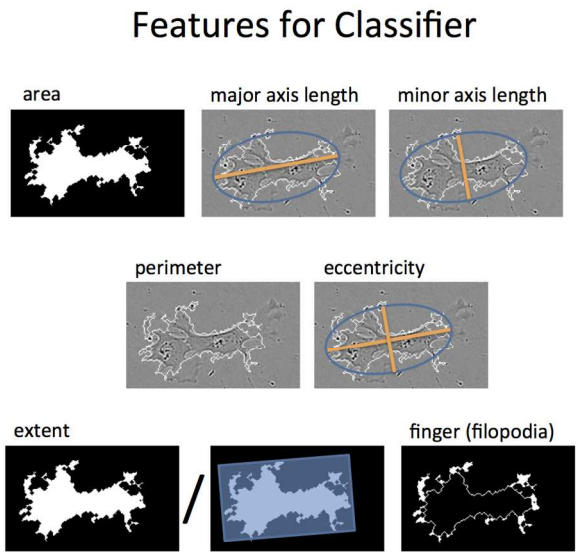

Figure 2. A-H Parameter space used to extract the features for the morphological analysis.

297x209mm (150 x 150 DPI)

Review

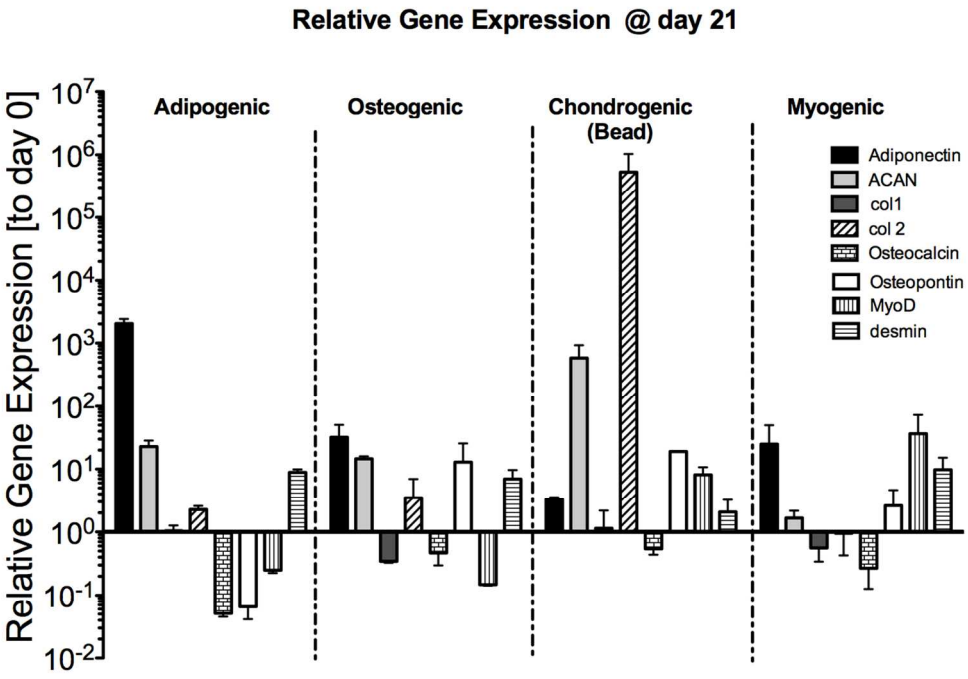

Figure 3. Relative gene expression profiles for marker genes grouped for osteogenic, adipogenic, chondrogenic and myogenic differentiation of human mesenchymal stem cells (hMSCs).
239x196mm (150 x 150 DPI)

view

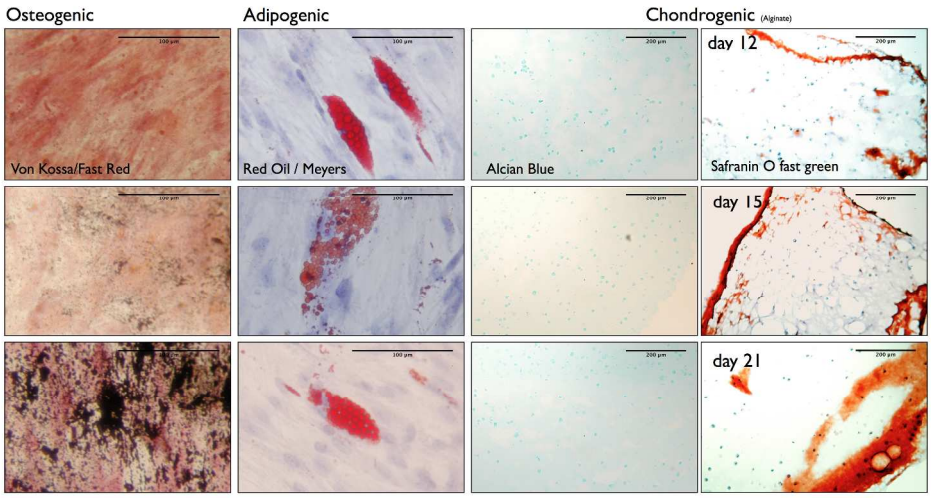

Figure 4. Histological stainings for each of the four differentiation lines of primary human mesenchymal stem cells after 12, 15 and 21 days. First, column: Osteogenic differentiation: Von Kossa /fast red stain, second column: adipogenic differentiation, red oils / Meyer's hematoxylin, third and forth column: chondrogenic differentiation aclian blue and safranin O / fast green stain.
1411x705mm (72 x 72 DPI)

er Review

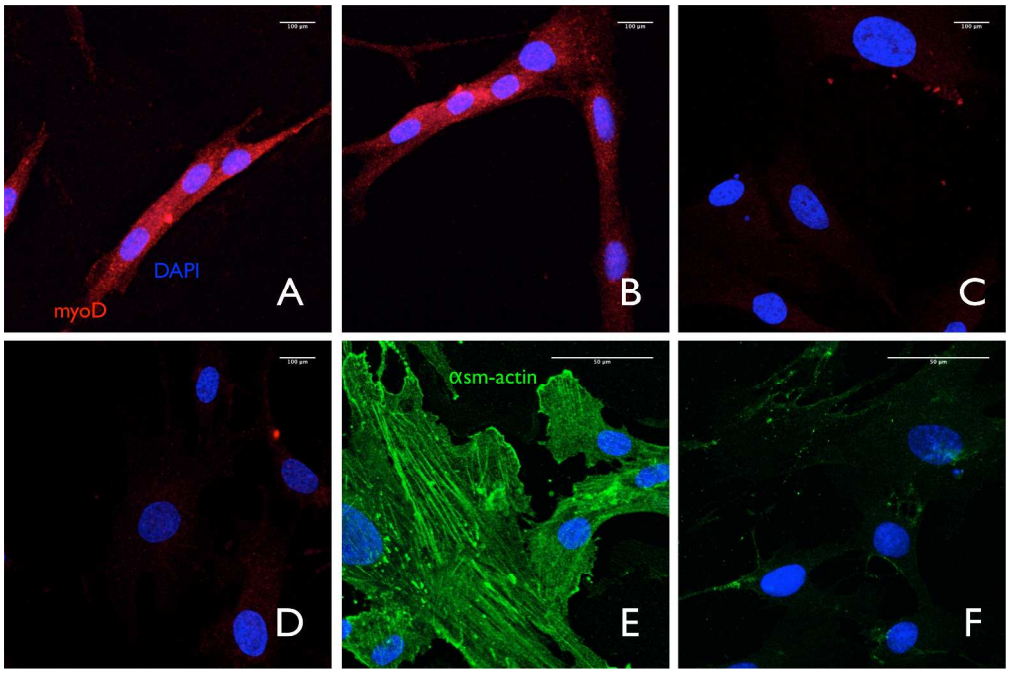

Figure 5. Confocal laser scanning microscope images of MyoD stain (ALEXA555) and for α-smooth muscle actin stain (FITC) for myogenic differentiation and negative controls. Nuclei were counter stained with DAPI. A. and B myotube formation after 14 days of culture which express MyoD, C is negative control and D is positive stain for undifferentiated control, E is positive staining for α smooth muscle (sm) actin of myogenic differentiation and F is negative control.
485x321mm (300 x 300 DPI)

For Review

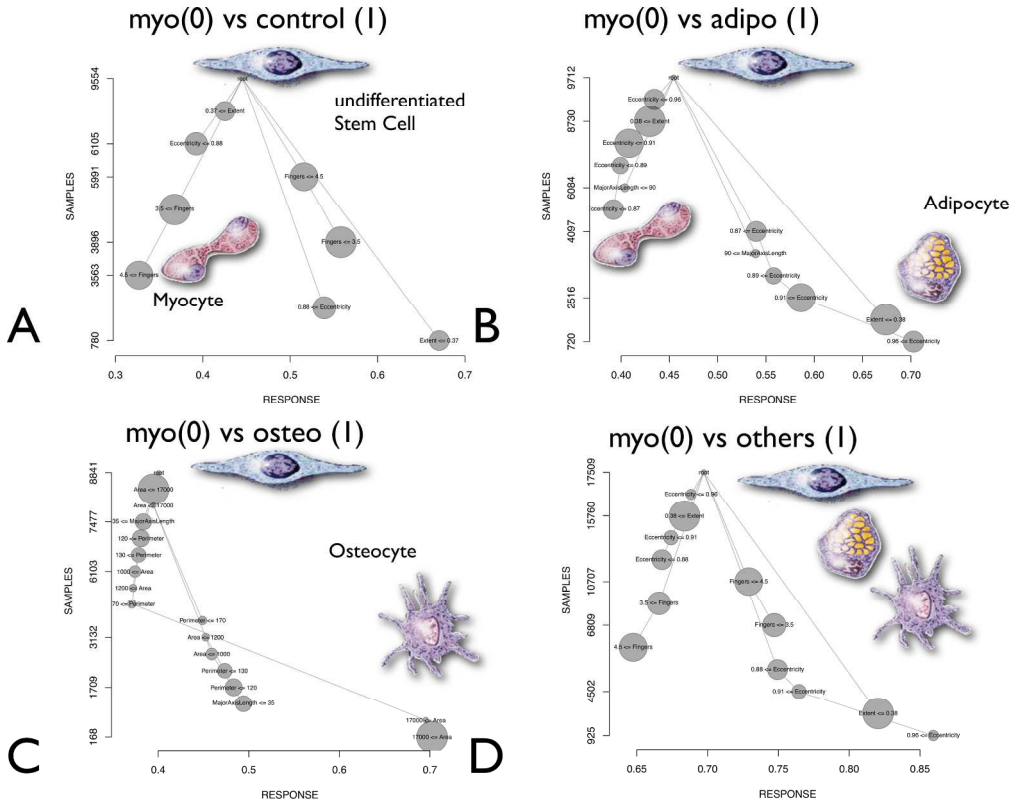

Figure 6. Output of Node Harvest classification method. The response axis represents A: myogenic=0 and control=1, B: myogenic=0 and adipogenic=1, C: myogenic=0 and osteogenic=1, D: myogenic=0 and adipgenic/osteogenic/control=1, where values between 0 and 1 represent a weighted combination of both types. The sample axis indicates the number of cells. Each node contains cells that fulfill one condition of one element of the 7-feature vector. The node size shows the relevance of that condition. Lines between nodes symbolize subsets.
205x162mm (300 x 300 DPI)